Microwave Sensor Dedicated to the Determination of the Dielectric Properties of 3D Biological Models from 500MHz to 20GHz

Olivia Peytral-Rieu, Katia Grenier, David Dubuc

Microwave Sensor Dedicated to the Determination of the Dielectric Properties of 3D Biological Models from 500MHz to 20GHz

Olivia Peytral-Rieu[#1], Katia Grenier[#2], David Dubuc[#3]

#LAAS-CNRS, Université de Toulouse, CNRS, UPS, Toulouse, France

[1]opeytral@laas.fr, [2]grenier@laas.fr, [3]dubuc@laas.fr

Abstract—**Biologists introduced some years ago an intermediate biological model between 2D cell culture and 3D *in vivo* tissues, called microtissues or spheroids. To study such 3D models, techniques are currently applied, including electromagnetic waves-based methods at low frequencies. This frequency range does not allow the penetration of the waves inside the cells, conversely to the microwaves. There is consequently a strong interest to develop an appropriate microwave-based sensor dedicated to microtissues analysis. This constitutes the topic of this paper with the introduction of a new microwave sensor, suitable for the dielectric characterization of microtissues. An analytic method is proposed to extract their electrical parameters. The evaluation of the biosensor is performed, while measuring large polystyrene beads with known dielectric properties, followed then by the dielectric evaluation of fixed spheroids from 500MHz to 20GHz.**

Keywords—**microwave biosensor, microtechnology, biological spheroids, microtissue.**

I. INTRODUCTION

Since the beginning of cancer study in the past century, biologists have been looking for in vitro biological models to analyse the living independently from in vivo investigations. 2D culture cells have therefore been used for long, due to their easiness in preparation and affordable cost. Such models are considered however quite far from the heterogeneity and the complexity of in vivo configuration. Mastered 3D cell aggregates, also called Multicellular Tumor Spheroids (MCTS), or microtissues, have consequently been introduced some years ago, constituting a new intermediate biological model between 2D and *in vivo* investigations [1]. They present both advantages of the 2D cell culture with rapidity of growing at an affordable cost, and the certain complexity of the in vivo configuration, while providing a physiological environment.

Different tools and techniques are used to study MCTS: mathematical modelling for growth study, optical microscopy for observation, protein and genes analyses with Western Blot and qRT-PCR, flow cytometry for viability kinetics for examples, and ElectroMagnetic (EM) Wave-based biosensors [2]. EM wave biosensors are interesting because they are non-invasive, non-destructive, label-free and cost-effective. Impedance spectroscopy (up to 1MHz) of MCTS enables the study of molecular exchange with the extracellular environment and membrane analysis [3]–[5]. This frequency range refers indeed to the β-dispersion, which corresponds to the phenomena related to the membrane polarization.
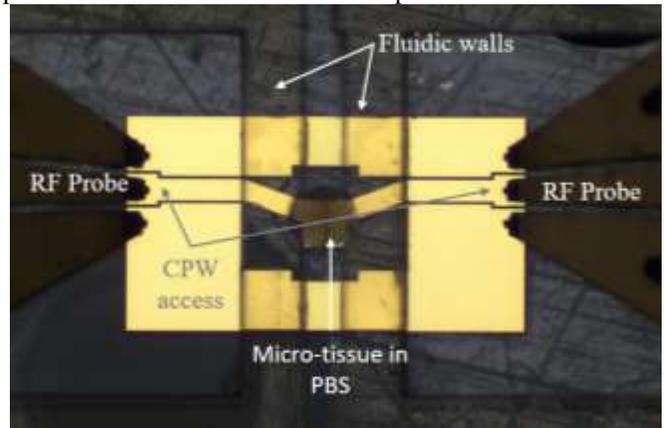

Fig. 1. Photography of the microwave sensor adapted to microtissue

In complementarity, microwave dielectric spectroscopy enables the electromagnetic waves to bypass the capacitive cellular membrane, leading to intracellular investigations. Various microwave based-devices already exist for the analysis of individual cells, cell suspensions, as well as for tissues and organs directly from patients [6]–[8]. However, to the best of our knowledge, none has been developed for this intermediate size of microtissues and this frequency range.

This article consequently presents a new micro-fabricated microwave (MW) biosensor suitable for the dielectric analysis of microtissues from 500MHz to 20GHz. An analytic method is developed to extract the electrical parameters of microtissues, followed by its exploitation with polystyrene beads and several microtissues.

II. MATERIALS AND METHODS

A. Microtissue: a 3D biological model

Traditionally, MCTS are used by biologists as they present strong cellular heterogeneity, constitutive regionalization with different cell layers, a necrotic heart, followed by living cells and quiescent ones. Growing is controllable, fast and affordable compare to animals with *in vivo* studies. Finally, strong interactions between cells exist inside the cell aggregates leading to more physiological cellular conditions.

This study is employing microtissues constituted of HEK293T cells. They are fixed using paraformaldehyde stored in Phosphate Buffer Solution (Gibco Phosphate Buffered Saline 1X in our case, called PBS in the rest of this article).

Due to microfabrication constraints, microtissues of around 360µm of diameter have been chosen for our experiments.

B. Architecture description of the biosensor and test setup

As shown with the photography of Fig.1, the microwave biosensor is composed of a coplanar waveguide with a capacitive gap located in the center of the structure. Coplanar accesses are widened to allow coplanar probes positioning with a pitch of 150 µm. The coplanar waveguide presents a capacitive gap of 10-µm width at the centre of the structure. The microtissue under test is localized just above this gap, within a fluidic reservoir. The fluidic walls permit to maintain the fixed microtissues in the PBS solution. All dimensions are given in Fig. 2. For the experiments, the fluidic channel is loaded with PBS solution. To characterize the fabricated microdevice up to 20 GHz, the device under test is connected to a Vector Network Analyser using two coplanar probes and two coaxial cables, using a preliminary SOLT calibration step.
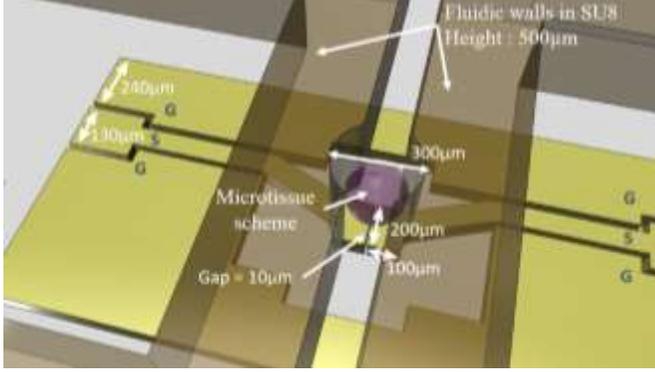

Fig. 2. Detailed schematic of the microwave sensor with a microtissue in its centre. S = Signal, G = Ground.

C. Microwave biosensor technology

The MW biosensor fabrication involves two main steps based on standard microtechnology processes. First the MW biosensor is realized on top of a flat alumina-borosilicate glass substrate, which has been preliminary cleaned with different chemical baths. The MW metallization is then performed using a lift-off technique. The obtained waveguide is composed of a flash of titanium to enable the metal adhesion on the substrate, followed by a gold layer of 0.3 µm thick. The 500 µm-thick fluidic walls are realized on top with SU8 resin.

D. Electrical model extraction method

As the MW biosensor is a two-port system, we have defined the electrical model of Fig. 3.
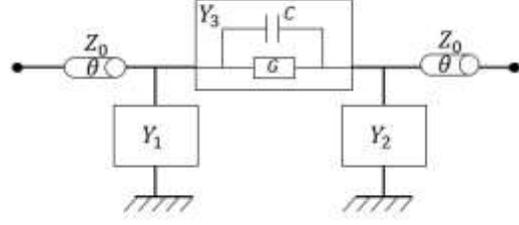

Fig. 3. Electric model of the device.

Y_3 is the admittance of our biological object under test, modelled by a capacitance C and a conductance G. Y_1 corresponds to the microfluidic channel admittances. Thanks to the theoretical classical formula, and for $\theta = 0°$, S parameters in this situation correspond to:

$$S_{11} = \frac{1 - 2y_1 y_3 - y_1^2}{(1+y_1)(1+y_1+2y_3)} \quad (1)$$

$$S_{21} = \frac{2y_3}{(1+y_1)(1+y_1+2y_3)} \quad (2)$$

where $y_x = Y_x Z_0$.

By adding Eq. (1) to Eq. (2), one may obtain Eq. (3).

$$y_1 = \frac{1 - (S_{11} + S_{21})}{1 + (S_{11} + S_{21})}; \quad (3)$$

By subtracting Eq. (2) to Eq. (3), y_3 may be written as

$$y_3 = \frac{2S_{21}}{(1+S_{11})^2 - S_{21}^2} \quad . \quad (4)$$

Nevertheless, Eq. (3) and Eq. (4) correspond to normalized admittances of the structure when $\theta = 0°$. The 2 coaxial cables located on each side of the device are also considered by adding two transmission lines, exhibiting a characteristic impedance Z_0. The measured S parameters become:

$$S_{11}' = S_{11} e^{-2j\theta} \quad (5)$$

$$S_{21}' = S_{21} e^{-2j\theta} \quad (6)$$

where j is the complex operator and θ is the electrical phase, which is considered identical on each side of the device due to its symmetry. By replacing S_{11} and S_{21} by their values issued from Eq. (5) and (6) into Eq. (3) and Eq. (4), we obtain:

$$y_1 = \frac{1 - (S_{11}' + S_{21}')e^{2j\theta}}{1 + (S_{11}' + S_{21}')e^{2j\theta}} \quad (7)$$

$$y_3 = \frac{2S_{21}' e^{2j\theta}}{(1 + S_{11}' e^{2j\theta})^2 - (S_{21}' e^{2j\theta})^2} \quad . \quad (8)$$

Assuming that when the device is empty (measurement performed at the beginning of the experiment), y_3 is equal to zero for $S_{11empty}'$ and $S_{21empty}'$ parameters. We obtain Eq. (9) by using Eq. (1) and Eq. (2):

$$e^{j2\theta} = \frac{1}{S_{11empty}'} \quad (9)$$

Finally, by applying Eq. (9) in Eq. (7) and Eq. (8), y_3 can be written as

$$y_3 = \frac{1}{2} \left(\frac{1 - \frac{S_{11}' - S_{21}'}{S_{11empty}'}}{1 + \frac{S_{11}' - S_{21}'}{S_{11empty}'}} - y_1 \right) \quad (10)$$

where

$$y_1 = \frac{1 - \frac{s_{11}' + s_{21}'}{s_{11empty}'}}{1 + \frac{s_{11}' + s_{21}'}{s_{11empty}'}}. \qquad (11)$$

Using the calculated y_3, one may extract the capacitance C and conductance G of our proposed electrical model of the biological object with Eq. (12) and Eq. (13) respectively.

$$C = \frac{1}{2\pi f} \frac{Img(y_3)}{50} \qquad (12)$$

$$G = \frac{Re(y_3)}{50} \qquad (13)$$

III. EVALUATION OF THE MW BIOSENSOR WITH A PBS SOLUTION, POLYSTYRENE BEADS AND 3D MICROTISSUES

As we are looking at weak electrical variations, while the sensor is loaded with the reference liquid (PBS in our case) and with beads, electrical contrasts are considered. Those capacitive and conductive contrasts are obtained using Eq. (14) and Eq. (15) respectively.

$$\Delta C = C_{DUT} - C_{PBS} \qquad (14)$$

$$\Delta G = G_{DUT} - G_{PBS} \qquad (15)$$

Where C_{DUT} and G_{DUT} are the capacitance and the conductance of device under test (loaded with an object or with PBS only for the control measurement) and C_{PBS} and G_{PBS} are the capacitance and the conductance obtained with PBS respectively. Each measurement is done during 27 min to observe and quantify potential measurement drift due to the open configuration of the fluidic reservoir. The first PBS measurement is used as the reference. Fig. 4 and Fig. 5 present the measured capacitive and conductive contrasts for PBS, different polystyrene beads and microtissues versus frequency and in the (ΔG, ΔC) plan respectively.
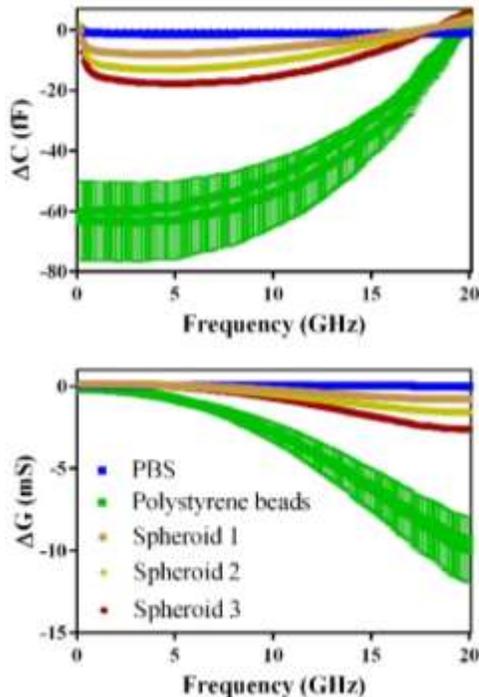

Fig. 4. Measured contrasts spectra obtained with the chosen reference fluid (PBS), polystyrene beads and fixed spheroids. Spheroid diameters are 262, 266

and 364µm respectively. The mean value and the standard deviation are represented (200 points/frequency sweep).

Microtissues exhibit low contrasts values compare to polystyrene beads. This is expected as the permittivity of cells is close to the one of PBS, due to strong water content, whereas polystyrene beads present a low permittivity value of 2.56. Moreover, as the used spheroids have been submitted to a paraformaldehyde fixation for the experiment, leading to the cell membrane permeabilization, fixed microtissues are constituted of dead cells. The expected contrasts with the host medium are even smaller as an equilibrium occurs between the extra and intracellular media [10]. Additionally, the largest capacitive contrast is obtained between 200 MHz and 5 GHz, instead of 20 GHz for the conductive contrast.
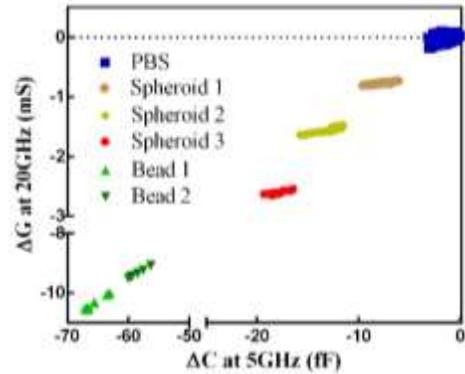

Fig. 5. Conductive contrast at 20 GHz versus capacitive contrast at 5 GHz of the PBS solution, polystyrene beads and three spheroids in PBS.

Taking now into consideration the standard deviations, the one of the beads in Fig. 4 is important for several reasons. First, the curve corresponds to the measurements of two different beads exhibiting diameters of 206 µm and 260 µm. Secondly, polystyrene beads are smaller than the hole in the fluidic channel, which is 300 µm large. Therefore, the exact position of the beads inside the hole is not well controlled with the actual sensor. Finally, a measurement drift slightly visible in Fig. 5 is observed with the PBS response, which is not exactly at the zero level. The drift may easily be explained by the evaporation occurring during the 27-minutes experiment with the open-fluidic sensor.

As far as microtissues are concerned, their deformability represents an advantage in comparison to polystyrene bead. It allows a better position control of the spheroids within the sensor, as noticeable in Fig. 1, which translates in less important standard deviations compare to beads. This confirms the significance of the object positioning in the device under test.

All these results are summarized in Table 1.

Table 1. Quantitative comparison between the different tested objects.

Object	ΔC at 5 GHz (fF)			ΔG at 20 GHz (mS)		
	Mean	SD	N	Mean	SD	N
Bead 1	- 63.03	12.89	23	- 9.948	2.00	23
Bead 2	- 58.52	1.260	6	- 9.339	0.144	6
Spheroid 1	- 8.040	0.961	24	- 0.775	0.022	24
Spheroid 2	- 13.09	1.274	26	- 1.556	0.049	26
Spheroid 3	- 17.83	0.769	16	- 2.600	0.029	16

IV. Conclusions

A microwave sensor enabling the RF characterization of microtissues is presented. The first measurements of fixed spheroids in a phosphate buffer saline solution in the frequency range of 500 MHz to 20 GHz are given. Even if optimizations of the device are required to further enhance the sensitivity and to avoid any drift (which are under development), this paper demonstrates the possible detection of 3D biological models, also called microtissues or spheroids, in the microwave range. This opens the door to new analyzing possibilities on a pertinent biological model, which avoids in vivo testing whereas exhibiting strong heterogeneity and complexity of the living.

Acknowledgment

References

[1] S. Nath et G. R. Devi, « Three-dimensional culture systems in cancer research: Focus on tumor spheroid model », *Pharmacol. Ther.*, vol. 163, p. 94-108, juill. 2016, doi: 10.1016/j.pharmthera.2016.03.013.

[2] E. C. Costa *et al*. « 3D tumor spheroids: an overview on the tools and techniques used for their analysis », *Biotechnol. Adv.*, vol. 34, nº 8, p. 1427-1441, déc. 2016, doi: 10.1016/j.biotechadv.2016.11.002.

[3] H. Thielecke *et al*., « Evaluation of impedance spectroscopy for the characterization of small biological samples in tissue-based test systems », in *The 26th Annual International Conference of the IEEE Engineering in Medicine and Biology Society*, San Francisco, CA, USA, 2004, vol. 3, p. 2070-2073, doi: 10.1109/IEMBS.2004.1403608.

[4] T. Gerasimenko *et al.*, « Impedance Spectroscopy as a Tool for Monitoring Performance in 3D Models of Epithelial Tissues », *Front. Bioeng. Biotechnol.*, vol. 7, p. 474, janv. 2020.

[5] R. Pethig et D. B. Kell, « The passive electrical properties of biological systems: their significance in physiology, biophysics and biotechnology », p. 38.

[6] M. Lazebnik *et al.*, « A large-scale study of the ultrawideband microwave dielectric properties of normal breast tissue obtained from reduction surgeries », *Phys. Med. Biol.*, vol. 52, nº 10, p. 2637-2656, mai 2007, doi: 10.1088/0031-9155/52/10/001.

[7] H. Li *et al.*, « Differentiation of live and heat-killed E. coli by microwave impedance spectroscopy », *Sens. Actuators B Chem.*, vol. 255, p. 1614-1622, févr. 2018, doi: 10.1016/j.snb.2017.08.179.

[8] A. Tamra *et al*. « Microwave dielectric spectroscopy for single cell irreversible electroporation monitoring », *2016 IEEE MTT-S Int. Microwave Symposium (IMS)*, San Francisco, CA, May 2016, p. 1-4.

[9] F. Artis *et al*., 'Microwaving biological cells - Intracellular analysis with microwave dielectric spectroscopy', IEEE Microwave Magazine, pp. 87-96, May 2015.